Acoustic axes in triclinic anisotropy

Václav Vavryčuk[a)]
Geophysical Institute, Academy of Sciences, Boční II/1401, 141 31 Praha 4, Czech Republic

(Received 12 November 2004; revised 9 May 2005; accepted 23 May 2005)

Calculation of acoustic axes in triclinic elastic anisotropy is considerably more complicated than for anisotropy of higher symmetry. While one polynomial equation of the 6th order is solved in monoclinic anisotropy, we have to solve two coupled polynomial equations of the 6th order in two variables in triclinic anisotropy. Furthermore, some solutions of the equations are spurious and must be discarded. In this way we obtain 16 isolated acoustic axes, which can run in real or complex directions. The real/complex acoustic axes describe the propagation of homogeneous/inhomogeneous plane waves and are associated with a linear/elliptical polarization of waves in their vicinity. The most frequent number of real acoustic axes is 8 for strong triclinic anisotropy and 4 to 6 for weak triclinic anisotropy. Examples of anisotropy with no or 16 real acoustic axes are presented. © *2005 Acoustical Society of America.* [DOI: 10.1121/1.1954587]

PACS number(s): 43.20.Bi, 43.35.Gk [ANN] Pages: 647–653

I. INTRODUCTION

Acoustic axes (singularities, degeneracies) in anisotropic media are the directions in which phase velocities of two or three plane waves coincide.[1–4] These directions are important in studying acoustic, seismic, or electromagnetic waves, because they cause anomalies in the field of polarization vectors,[5,6] and they are associated with energy focusing due to caustics in the wave surface.[7–14] Acoustic axes also pose complications in tracing rays[15,16] and in wave field modeling because of coupling of waves.[17–22]

Acoustic axes form single isolated points on the slowness surface, or they join into lines. The isolated acoustic axes can exist in all anisotropy symmetries, the line acoustic axes typically occur in transverse isotropy. The maximum number of isolated acoustic axes is:[23–31] 16 in monoclinic, orthorhombic, and trigonal symmetry, 13 in tetragonal symmetry, 7 in cubic symmetry, and 1 in transverse isotropy. The directions of the acoustic axes in the mentioned symmetries are calculated by solving polynomial equations in one variable. The highest degree of the polynomials is 6 for monoclinic symmetry, or less for other symmetries, hence solving the polynomials numerically does not pose any difficulty. However, as regards triclinic anisotropy, the problem is more involved. Khatkevich[23] proved that the acoustic axes in triclinic anisotropy can be calculated by solving two polynomial equations of the 6th order in two variables. This implies that the number of acoustic axes in triclinic anisotropy cannot exceed 36. However, Khatkevich[23] did not discuss whether the actual maximum number of acoustic axes is less than 36 or not. Later on, Darinskii[28] proved that typical triclinic anisotropy (when $S1$ and $S2$ waves are degenerate) cannot have more than 16 acoustic axes, and Holm[27] proved that generic triclinic anisotropy (anisotropy with stable acoustic axes) also possess no more than 16 acoustic axes. Here it is proved that the maximum number of acoustic axes is 16 under no restrictions on triclinic anisotropy. Several approaches to determining the acoustic axes in triclinic anisotropy are presented and it is discussed which scheme is optimum for numerical calculations. Examples of triclinic anisotropy with no and 16 acoustic axes are presented, and the most frequent number of acoustic axes in triclinic media and its dependence on anisotropy strength is investigated.

II. THEORY

The Christoffel tensor $\mathbf{\Gamma}(\mathbf{n})$ is defined as[20,24,32]

$$\Gamma_{jk}(\mathbf{n}) = a_{ijkl} n_i n_l, \tag{1}$$

where a_{ijkl} are the density-normalized elastic parameters and $\mathbf{n}$ is the unit vector defining the slowness direction. The Einstein summation convention over repeated subscripts is applied. The elastic parameters a_{ijkl} must satisfy the stability conditions, if the medium is to be physically realizable:

$$a_{11} > 0, \quad \begin{vmatrix} a_{11} & a_{12} \\ a_{12} & a_{22} \end{vmatrix} > 0,$$

$$\begin{vmatrix} a_{11} & a_{12} & a_{13} \\ a_{12} & a_{22} & a_{23} \\ a_{13} & a_{23} & a_{33} \end{vmatrix} > 0, \ldots, \det(a_{\alpha\beta}) > 0, \tag{2}$$

where the two-index Voigt notation $a_{\alpha\beta}$, $\alpha, \beta = 1, \ldots, 6$ has been used [see Musgrave,[32] Eq. (3.13.4)]. These conditions correspond to the requirement that the strain energy of the medium must be positive [see Payton,[33] Eqs (1.4.3.) and (1.4.4)].

The Christoffel tensor $\mathbf{\Gamma}(\mathbf{n})$ has three eigenvalues $G^{(M)}$ and three unit eigenvectors $\mathbf{g}^{(M)}$, which are calculated from

$$\Gamma_{jk} g_k^{(M)} = G^{(M)} g_j^{(M)}, \quad M = 1,2,3, \tag{3}$$

where M denotes the type of the wave (P, $S1$, or $S2$). The eigenvalues correspond to the squared phase velocities, $G = c^2$, and the eigenvectors describe the polarization vectors of the waves.

Acoustic axes are defined as the directions in which two eigenvalues of the Christoffel tensor coincide

[a)]Electronic mail: vv@ig.cas.cz

$$G^{(1)}(\mathbf{n}) = G^{(2)}(\mathbf{n}) \neq G^{(3)}(\mathbf{n}), \tag{4}$$

and thus the Christoffel tensor is degenerate. Exceptionally, all three eigenvalues can coincide

$$G^{(1)}(\mathbf{n}) = G^{(2)}(\mathbf{n}) = G^{(3)}(\mathbf{n}), \tag{5}$$

but this type of the acoustic axis is unstable and very rare.

In the following, I will present three different approaches to determining acoustic axes in anisotropic media: the Fedorov approach[24] based on solving one 12th-order multivariate polynomial equation, the Khatkevich approach[23] based on solving two 6th-order multivariate polynomial equations, and the Darinskii approach[28] based on solving six multivariate quadratic equations.

A. The Fedorov equation

Calculating the eigenvalues G of the Christoffel tensor $\mathbf{\Gamma}(\mathbf{n})$ from

$$\det(\Gamma_{jk} - G\delta_{jk}) = 0, \tag{6}$$

we obtain the following cubic equation:

$$G^3 - PG^2 + QG - R = 0, \tag{7}$$

where P, Q, and R are invariants of $\mathbf{\Gamma}(\mathbf{n})$,

$$P = \Gamma_{11} + \Gamma_{22} + \Gamma_{33}, \tag{8}$$

$$Q = \Gamma_{11}\Gamma_{22} + \Gamma_{11}\Gamma_{33} + \Gamma_{22}\Gamma_{33} - \Gamma_{12}^2 - \Gamma_{13}^2 - \Gamma_{23}^2, \tag{9}$$

$$R = \Gamma_{11}\Gamma_{22}\Gamma_{33} + 2\Gamma_{12}\Gamma_{13}\Gamma_{23} - \Gamma_{11}\Gamma_{23}^2 - \Gamma_{22}\Gamma_{13}^2 - \Gamma_{33}\Gamma_{12}^2. \tag{10}$$

The cubic equation (7) has three real roots, of which at least two are equal, if [see Fedorov,[24] Eq. (18.18)]

$$4P^3R - P^2Q^2 - 18PQR + 4Q^3 + 27R^2 = 0. \tag{11}$$

Equation (11) is the 12th-order homogeneous polynomial equation in three unknowns n_1, n_2, and n_3. It has an infinite number of complex-valued solutions, but the number of real-valued solutions is finite.

B. The Darinskii equations

Using the spectral decomposition of $\mathbf{\Gamma}(\mathbf{n})$

$$\Gamma_{jk} = G^{(1)}g_j^{(1)}g_k^{(1)} + G^{(2)}g_j^{(2)}g_k^{(2)} + G^{(3)}g_j^{(3)}g_k^{(3)}, \tag{12}$$

and applying the condition for the acoustic axis, $G^{(2)}=G^{(3)}$, we obtain

$$\Gamma_{jk} = (G^{(1)} - G^{(2)})g_j^{(1)}g_k^{(1)} + G^{(2)}\delta_{jk}, \tag{13}$$

where δ_{jk} is the Kronecker delta and the following identity was used:

$$\delta_{jk} = g_j^{(1)}g_k^{(1)} + g_j^{(2)}g_k^{(2)} + g_j^{(3)}g_k^{(3)}. \tag{14}$$

If $G^{(1)} > G^{(2)} = G^{(3)}$, the $S1$ and $S2$ phase velocities coincide at the acoustic axis, if $G^{(1)} < G^{(2)} = G^{(3)}$, the P and $S1$ phase velocities coincide at the acoustic axis. Equation (13) can be expressed as follows [see Darinskii,[28] Eq. (4)]:

$$a_{ijkl}s_is_l = g_jg_k + \delta_{jk}, \tag{15}$$

where $\mathbf{s}=\mathbf{n}/\sqrt{G^{(2)}}$ is the slowness vector of the degenerate wave and $\mathbf{g}=\mathbf{g}^{(1)}\sqrt{(G^{(1)}-G^{(2)})/G^{(2)}}$ is an eigenvector of the nondegenerate wave of a generally nonunit length. The vectors $\mathbf{s}$ and $\mathbf{g}$ may be real- or complex-valued. Equation (15) is a system of six quadratic equations for six unknowns: $\mathbf{s}=(s_1,s_2,s_3)^T$ and $\mathbf{g}=(g_1,g_2,g_3)^T$. The number of solutions is $2^6=64$. If we take into account that solutions of different signs: $\pm\mathbf{s}$, $\pm\mathbf{g}$, correspond to the same acoustic axis, the maximum number of acoustic axes is reduced from 64 to 16. This number comprises acoustic axes with real-valued as well as complex-valued slowness vector $\mathbf{s}$.

C. The Khatkevich equations

Eliminating eigenvalues and eigenvectors in Eq. (13), we obtain:[28]

$$\Gamma_{11} - \frac{\Gamma_{12}\Gamma_{13}}{\Gamma_{23}} = \Gamma_{22} - \frac{\Gamma_{12}\Gamma_{23}}{\Gamma_{13}} = \Gamma_{33} - \frac{\Gamma_{13}\Gamma_{23}}{\Gamma_{12}}, \tag{16}$$

and subsequently [see Khatkevich,[23] Eq. (11)]

$$(\Gamma_{11} - \Gamma_{22})\Gamma_{13}\Gamma_{23} - \Gamma_{12}(\Gamma_{13}^2 - \Gamma_{23}^2) = 0, \tag{17a}$$

$$(\Gamma_{11} - \Gamma_{33})\Gamma_{12}\Gamma_{23} - \Gamma_{13}(\Gamma_{12}^2 - \Gamma_{23}^2) = 0, \tag{17b}$$

$$(\Gamma_{22} - \Gamma_{33})\Gamma_{12}\Gamma_{13} - \Gamma_{23}(\Gamma_{12}^2 - \Gamma_{13}^2) = 0. \tag{17c}$$

Equations (17a)–(17c) represent a system of 6th-order equations for three unknown components of the unit direction vector $\mathbf{n}$: n_1, n_2, and n_3. The three equations [(17a)–(17c)] are not independent, hence we solve only two of them. We obtain 72 solutions, which are generally complex-valued. Taking into account that $\pm\mathbf{n}$ describes the same direction, the number of directions reduces from 72 to 36.

Since Eq. (15) yields only 16 acoustic axes, 20 of the 36 directions calculated from Eqs. (17) must be spurious and do not describe acoustic axes. In fact, the spurious directions were incorporated into the solution, when Eq. (16) was multiplied by terms $\Gamma_{12}\Gamma_{13}$, $\Gamma_{12}\Gamma_{23}$ or $\Gamma_{13}\Gamma_{23}$ in order to derive Eqs. (17). Therefore, we should eliminate from the solutions of Eqs. (17a)–(17c), the directions for which

$$\Gamma_{13} = 0, \quad \Gamma_{23} = 0, \tag{18a}$$

or

$$\Gamma_{12} = 0, \quad \Gamma_{23} = 0, \tag{18b}$$

or

$$\Gamma_{12} = 0, \quad \Gamma_{13} = 0. \tag{18c}$$

Equations (18a)–(18c) describe three systems of quadratic equations, each of them having 8 solutions which reduce to 4 directions when omitting different signs of $\mathbf{n}$. Hence, we obtained a total of 12 spurious directions. Furthermore, 8 of the 12 spurious directions appear in Eqs. (17) twice. Which 8 spurious directions are doubled, depends on the pair of Eqs. (17a)–(17c) we actually solve. For example, when solving

Eqs. (17a) and (17b), the solutions of Eqs. (18a) and (18b) are doubled, when solving Eqs. (17b) and (17c), the solutions of Eqs. (18b) and (18c) are doubled. Hence, the total number of spurious directions in Eqs. (17) is 20. This confirms that only 16 acoustic axes can exist in triclinic anisotropy.

III. NUMERICAL CALCULATION OF ACOUSTIC AXES

In principal, all three above-mentioned approaches can be used for determining acoustic axes in triclinic anisotropy. However, they are differently efficient from the point of view of programming and numerics. The numerical tests show that the acoustic axes in triclinic anisotropy can be conveniently calculated using the Khatkevich approach, because it represents a standard problem of solving two polynomial equations in two unknowns. The Darinskii approach requires elaborating with higher number of equations, and the Fedorov approach yields real-valued acoustic axes but not complex-valued acoustic axes (for details, see Sec. IV). Moreover, the Fedorov approach is rather untypical, because we have to solve one polynomial equation in two unknowns.

The Khatkevich equations (17a)–(17c) are homogeneous polynomial equations of the 6th order in three unknown components n_1, n_2, and n_3 of the unit direction vector $\mathbf{n}$. Using the substitutions $u=n_1/n_3$ and $v=n_2/n_3$, we obtain inhomogeneous polynomial equations of the 6th order in unknowns u and v. The roots of the equations can be calculated, for example, using Gröbner bases,[34] implemented in symbolic algebra packages. Solving Eqs. (17a)–(17c) we obtain 36 solutions, from which we have to exclude 20 spurious solutions defined by Eqs. (18a)–(18c). To identify and eliminate the spurious solutions, we can either solve Eqs. (18a)–(18c) or we can simply check at which of the 36 directions calculated from Eqs. (17a)–(17c) the Christoffel tensor is nondegenerate. Using this approach, we obtain real as well as complex acoustic axes in triclinic anisotropy. For anisotropy of higher symmetry, it is not convenient to use this approach, because it is too complex and it may even fail when the true or spurious solutions are not isolated. Instead, much simpler systems of algebraic equations designed for each specific symmetry are used.[23,29] Equations (17a)–(17c) can also fail when triclinic anisotropy is extremely weak. In this case, the left-hand sides of Eqs. (17a)–(17c) are very close to zero for all directions $\mathbf{n}$, hence the solution can be distorted by numerical errors.

Finally, I should also mention a possibility to calculate acoustic axes using a direct numerical approach. This approach is based on minimizing the square of the difference between numerically calculated eigenvalues of the Christoffel tensor. The minimization can be performed using some standard inversion technique like the gradient method. Since the misfit function has several minima, we have to invert repeatedly for varying initial guesses of the position of the acoustic axis. Not to skip some solutions, the initial positions of the acoustic axes should cover the whole hemisphere in a regular grid and the grid should be sufficiently dense. This approach is applicable to any type of anisotropy and is also reasonably fast. However, it does not yield complex acoustic axes and sometimes it may skip some solutions, for example, in situations when two acoustic axes are very close each to the other.

IV. REAL- AND COMPLEX-VALUED ACOUSTIC AXES

As mentioned earlier, the 16 acoustic axes in triclinic anisotropy can lie along a real-valued or complex-valued direction $\mathbf{n}$. The real-valued acoustic axis corresponds to the propagation of a homogeneous plane wave:

$$u_k(\mathbf{x},t) = Ag_k \exp[-i\omega(t - s_j x_j)], \tag{19}$$

where $\mathbf{u}$ is the real-valued displacement, A is the scalar real- or complex-valued amplitude, and $\mathbf{s}=\mathbf{n}/\sqrt{G}$ is the real-valued slowness vector. Since the Christoffel tensor $\mathbf{\Gamma}$ and its eigenvalues G and eigenvectors $\mathbf{g}$ are real-valued, the polarization near the acoustic axis is linear. Strictly at the singularity, the polarization is not defined because of the degeneracy of $\mathbf{\Gamma}$.

If the acoustic axis is complex-valued, the corresponding plane wave solution describes an inhomogeneous wave:

$$\begin{aligned} u_k(\mathbf{x},t) &= Ag_k \exp[-i\omega(t - s_j x_j)] \\ &= Ag_k \exp(-a_j x_j)\exp[-i\omega(t - p_j x_j)], \end{aligned} \tag{20}$$

where A is the scalar real- or complex-valued amplitude, $\mathbf{s}$ is the complex-valued slowness vector, $\mathbf{s}=\mathbf{n}/\sqrt{G}=\mathbf{p}+i\mathbf{a}$, and $\mathbf{p}$ and $\mathbf{a}$ are the real-valued propagation and attenuation vectors.[35] Subsequently, the Christoffel tensor $\mathbf{\Gamma}$ and its eigenvalues G and eigenvectors $\mathbf{g}$, calculated by Eqs. (1) and (3), are complex-valued, and the polarization near the acoustic axis is elliptical. The ellipticity depends on the direction and magnitude of attenuation vector $\mathbf{a}$. Similarly as for homogeneous waves, the polarization is not defined at the acoustic axis because of the degeneracy of $\mathbf{\Gamma}$. Since the problem of degeneracy is more involved for complex-valued tensors than for real-valued tensors, Eqs. (15) and (17) do not describe all acoustic axes for inhomogeneous waves, but only the so-called "semisimple" axes (degeneracies). The "nonsemisimple" degneracies cannot be investigated by these equations. For more details about the semisimple and nonsemisimple degeneracies, see Ting[36] and Shuvalov.[37]

The polarization properties of homogeneous and inhomogeneous waves near real and complex acoustic axes are exemplified for triclinic anisotropy generated from an isotropic medium with $\lambda=1$, $\mu=1$, by adding small perturbations. The elastic parameters are as follows:

$$\mathbf{A} = \begin{bmatrix} 3.004 & 1.004 & 1.004 & 0.004 & 0.002 & -0.001 \\ & 3.004 & 1.002 & -0.002 & -0.001 & 0.001 \\ & & 3.000 & 0.003 & -0.001 & 0.004 \\ & & & 1.001 & 0.001 & -0.001 \\ & & & & 1.000 & 0.003 \\ & & & & & 1.000 \end{bmatrix}. \tag{21}$$

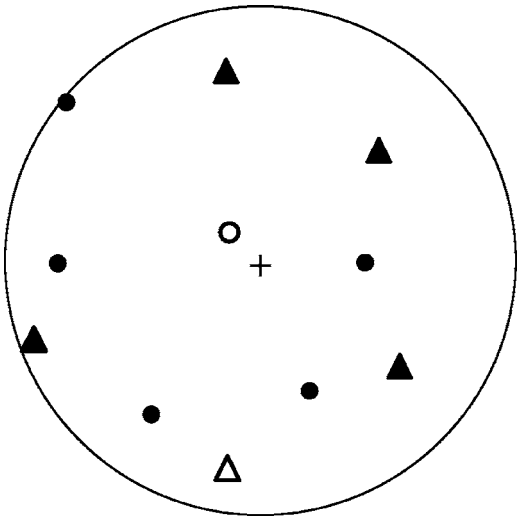

FIG. 1. Positions of real (circles) and complex (triangles) acoustic axes for triclinic anisotropy described by Eq. (21). The plus sign marks the vertical axis. The open circle and open triangle show the acoustic axes, for which the polarization field in their vicinities is shown in Figs. 2 and 3. Equal-area projection is used.

The positions of the acoustic axes over the unit sphere are shown in Fig. 1. The medium contains 6 real and 10 complex acoustic axes. For complex axes, their positions on the sphere are calculated from the real parts of complex directions **n**. Since the complex axes always appear in complex conjugate pairs, Fig. 1 shows 5 instead 10 positions. Figure 2 shows the polarization of homogeneous waves near the real acoustic axis marked in Fig. 1 by an open circle. The field of polarization vectors displays a singularity with the topological charge $-1/2$. Figure 3 shows the polarization of inhomogeneous waves near the complex acoustic axis marked in Fig. 1 by an open triangle. The field of polarization vectors displays a singularity with the topological charge $+1/2$.

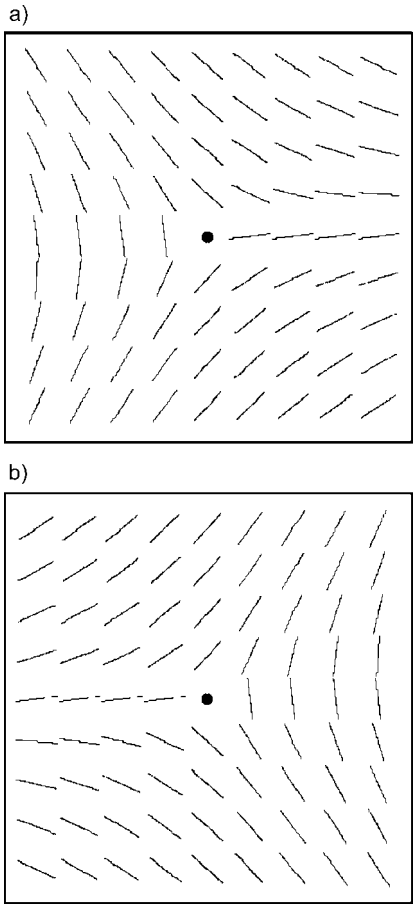

FIG. 2. Polarization field near a real acoustic axis for (a) $S1$ wave, and (b) $S2$ wave. The topological charge is $-1/2$. The dot marks the position of the acoustic axis.

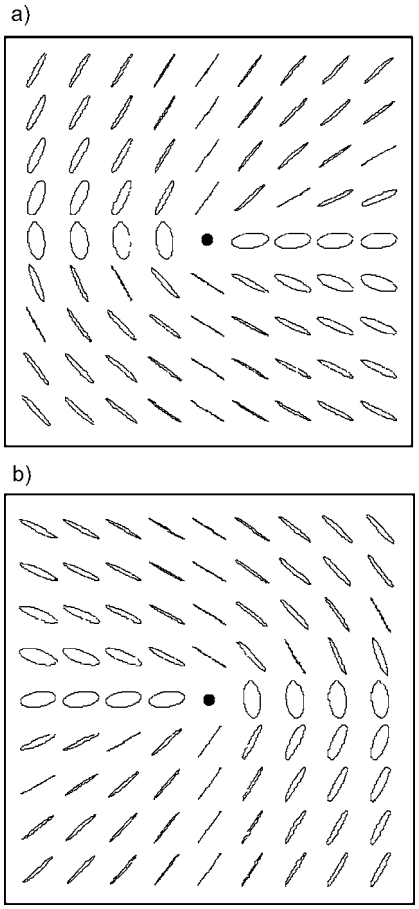

FIG. 3. Polarization field near a complex acoustic axis for (a) $S1$ wave, and (b) $S2$ wave. The topological charge is $+1/2$. The dot marks the position of the acoustic axis.

V. STABLE AND UNSTABLE ACOUSTIC AXES

Acoustic axes can be either single or multiple. The single/multiple acoustic axis corresponds to a nondegenerate/degenerate solution of Eqs. (17a)–(17c). The single axis is stable, because it cannot split or disappear under a small perturbation of elastic parameters. The axis only slightly changes its direction. The multiple axis is unstable, because a small perturbation of elastic parameters removes its degeneracy and splits the axis into two or more single axes. The real-valued multiple axis can split into real-valued and/or complex-valued single axes. The topological charge of the multiple real acoustic axis is equal to the sum of the topological charges of split single real axes.[28]

The properties of the multiple acoustic axes will be exemplified on a transition from cubic to triclinic anisotropy by a small perturbation of elastic parameters. The cubic anisotropy is characterized by 4 single real-valued axes in the directions $\langle \pm 1, \pm 1, \pm 1 \rangle$ and three multiple real-valued axes $\langle \pm 1, 0, 0 \rangle$, $\langle 0, \pm 1, 0 \rangle$, and $\langle 0, 0, \pm 1 \rangle$. The multiple axes are 4 times degenerate. The total number of real-valued acoustic axes is 7. However, if we consider multiplicities, we obtain 16 real-valued axes, which is the maximum number of acoustic axes in anisotropy. This implies that no other complex-valued axis can exist in cubic anisotropy. The topological charge of each multiple axis is +1. If we perturb elastic parameters from cubic to triclinic anisotropy, the single axes slightly change their directions and each multiple axis splits into two real-valued and two complex-valued single axes. Each split real-valued single axis has a topological charge of +1/2.

VI. FREQUENCY OF ACOUSTIC AXES

Now let us address the problem of the balance between the numbers of real- and complex-valued acoustic axes, and how this balance depends on the strength of anisotropy. The number of real and complex acoustic axes will be studied numerically on randomly generated triclinic anisotropy. The triclinic anisotropy with elastic parameters a_{ijkl} is obtained by perturbing an isotropic medium in the following way:

$$a_{ijkl} = a^0_{ijkl} + \varepsilon a^1_{ijkl}, \tag{22}$$

where

$$a^0_{ijkl} = \lambda \delta_{ij}\delta_{kl} + \mu(\delta_{ik}\delta_{jl} + \delta_{il}\delta_{jk}). \tag{23}$$

Parameters λ and μ define the Lamé coefficients of an isotropic medium, tensor a^1_{ijkl} defines perturbations into triclinic anisotropy, and ε is a measure of the anisotropy strength. Parameters λ and μ are fixed at values $\lambda=1$, $\mu=1$, perturbations a^1_{ijkl} are generated randomly with a uniform nonzero probability in the interval $\langle -3, 3 \rangle$, and ε is 0.01 or 1. The generated triclinic media were checked to stability using Eq. (2), and the unstable media were discarded. For $\varepsilon=0.01$, all the media were stable, for $\varepsilon=1$, approximately one hundredth of the media were stable. To obtain statistically relevant results, the number of randomly generated stable triclinic media is 1000 for each ε.

Figure 4 shows the frequency of occurrence of acoustic axes in the studied triclinic media. The figure shows that the number of acoustic axes depends on the strength of anisotropy. For weak anisotropy, defined by $\varepsilon=0.01$, the randomly generated triclinic anisotropy contains most frequently 4 to 6 real and 10 to 12 complex axes. For strong anisotropy, defined by $\varepsilon=1$, the most frequent number is 8 real and 8 complex axes. Media with no real or no complex axis are admissible, but they are very rare. To demonstrate their existence, elastic parameters of two media are presented in Table I: anisotropy I with 16 real axes, and anisotropy II with 16 complex axes. Figure 5 shows the distribution of axes over the sphere. For complex axes, their positions on the sphere are calculated from the real parts of complex directions **n**. Since the complex axes always appear in complex conjugate pairs, Fig. 5(b) shows 8 instead 16 positions. Anisotropy I was generated in a similar way as other randomly generated triclinic media in the above-described numerical tests. Anisotropy II was derived from orthorhombic anisotropy with no real acoustic axes, presented by Boulanger and Hayes[29] by perturbing it into the triclinic anisotropy.

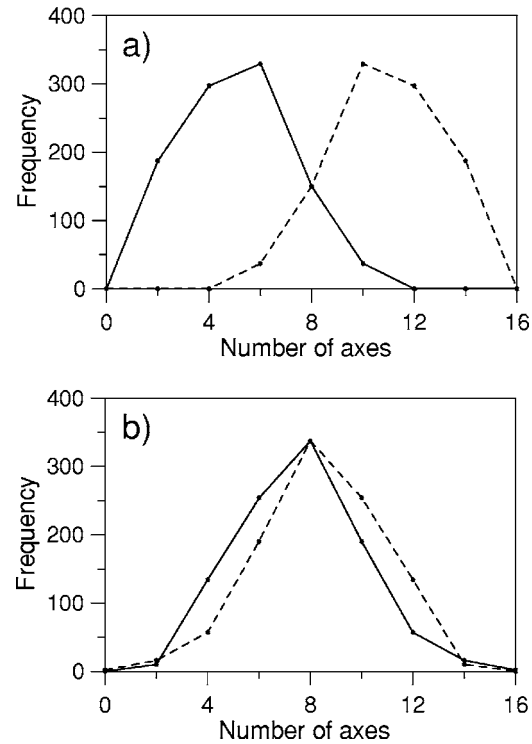

FIG. 4. Frequency of occurrence of real (solid line) and complex (dashed line) acoustic axes in randomly generated triclinic anisotropy with strength: (a) $\varepsilon=0.01$, and (b) $\varepsilon=1$.

VII. POSITIONS OF ACOUSTIC AXES AS A FUNCTION OF ANISOTROPY STRENGTH

Here, variations in positions of acoustic axes will be studied in dependence on anisotropy strength. The variations will be shown on two examples of triclinic anisotropy de-

TABLE I. Examples of triclinic anisotropy with 16 real and 16 complex acoustic axes.

	a_{11}	a_{12}	a_{13}	a_{14}	a_{15}	a_{16}	a_{22}	a_{23}	a_{24}	a_{25}	a_{26}	a_{33}	a_{34}	a_{35}	a_{36}	a_{44}	a_{45}	a_{46}	a_{55}	a_{56}	a_{66}
I[a]	137	52	57	−13	32	−20	147	18	−6	20	−9	100	22	−15	5	52	26	−7	75	−40	30
II[b]	31	−5	−32	2	−2	−3	9	−11	2	5	4	90	5	−1	−2	12	1	−3	35	−2	10

[a]I—anisotropy with 16 real acoustic axes.
[b]II—anisotropy with 16 complex acoustic axes.

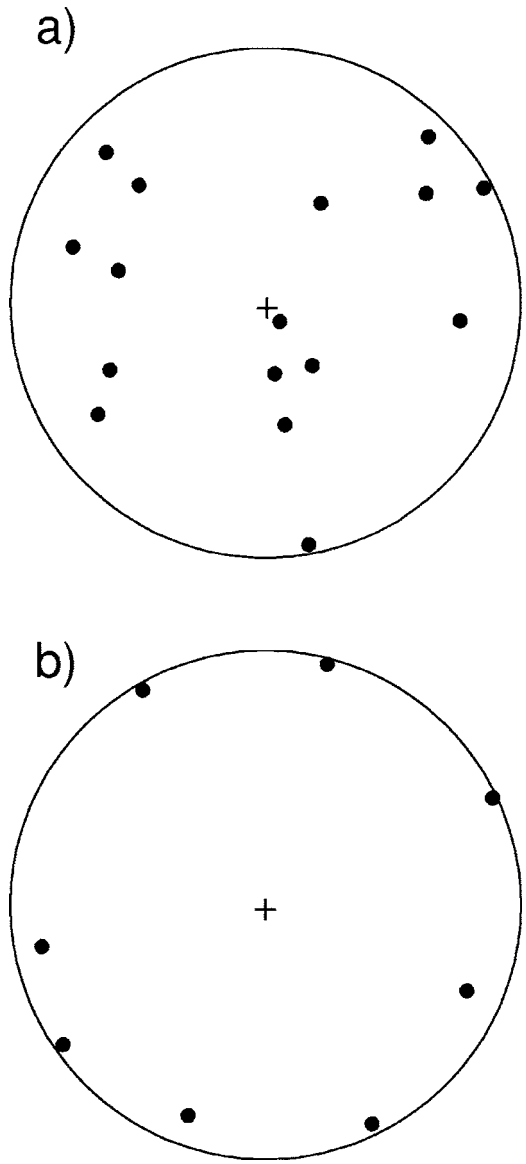

FIG. 5. Positions of acoustic axes in: (a) anisotropy I with 16 real and no complex acoustic axes, and (b) anisotropy II with 16 complex and no real acoustic axes. The acoustic axes are marked by dots, the vertical axis is marked by the plus sign. Equal-area projection is used. Note that the near-horizontal directions of all complex acoustic axes in (b) are rather untypical and not frequently observed.

fined by the Lamé coefficients of the isotropic background medium $\lambda=1$, $\mu=1$, and by the perturbations a^1_{ijkl}:

$$\mathbf{A}^1=\begin{bmatrix} 1.083 & 1.200 & 0.966 & 0.954 & 0.483 & -0.474 \\ & 1.062 & 0.435 & -0.630 & -0.474 & 0.105 \\ & & 0.000 & 0.684 & -0.570 & 1.017 \\ & & & 0.282 & 0.207 & -0.387 \\ & & & & -0.009 & 0.609 \\ & & & & & 0.000 \end{bmatrix}, \tag{24}$$

$$\mathbf{A}^1=\begin{bmatrix} -0.114 & 0.309 & -1.347 & -0.585 & 1.125 & -1.452 \\ & 0.204 & -0.252 & 0.804 & 1.413 & 1.473 \\ & & 0.000 & 0.867 & -0.183 & -0.003 \\ & & & 0.885 & -0.858 & 0.432 \\ & & & & -1.320 & -0.537 \\ & & & & & 0.000 \end{bmatrix}. \tag{25}$$

The anisotropy strength ε ranged from -1000 to 1000 with a varying step. The step was small enough to map densely changes in the directions of acoustic axes. Figure 6 shows the positions of the real acoustic axes in the equal-area projection. The blue/red points mark the axes for stable/unstable media. The figure shows that: (1) The positions of the acoustic axes depend on strength of anisotropy. (2) The acoustic axes are not distributed randomly around a sphere but form a complicated line which can intersect itself. Some segments of the line correspond to the acoustic axes of stable media, the other segments correspond to the axes of unstable media. (3) For high absolute values of ε, the directions of acoustic axes become insensitive to anisotropy strength, and for ε close to ± 1000, the positions of the acoustic axes are almost constant. (4) Since the acoustic axes for $\varepsilon \rightarrow \pm\infty$ coincide, the line is closed.

The complex acoustic axes display a similar pattern. Obviously, for anisotropy of higher symmetry, the form of the line simplifies.

VIII. CONCLUSIONS

The acoustic axes in triclinic anisotropy can be conveniently calculated by solving two coupled polynomial equations of the 6th order in two unknowns. From the 36 directions obtained, 20 of them are spurious and must be eliminated. The spurious directions are solutions of three systems of quadratic equations in two unknowns. Hence, the maximum number of isolated acoustic axes in triclinic anisotropy is 16. These axes can be real or complex, and single or multiple. If we count both real and complex acoustic axes and their multiplicities, the total number of isolated axes is always 16 regardless of symmetry or strength of anisotropy. The real axes correspond to the degeneracy directions of the real-valued Christoffel tensor, which describes the propagation of homogeneous plane waves. The complex axes correspond to the semisimple degeneracy directions of the complex-valued Christoffel tensor which describes the propagation of inhomogeneous plane waves. The inhomogeneous waves can also possess other types of acoustic axes called nonsemisimple. The real-valued acoustic axis is associated with a linear polarization in its vicinity, which is singular at the axis. The complex-valued (semisimple) acoustic axis is associated with an elliptical polarization, which is also singular at the axis. Numerical simulations indicate that the most frequent number of real acoustic axes is only 4 to 6 for weak anisotropy and 8 for strong anisotropy. A medium with no or 16 real acoustic axes is admissible, but it is very rare. Positions of the acoustic axes depend on strength of anisotropy. If we fix the perturbation matrix a^1_{ijkl} and change anisotropy strength ε, the positions of acoustic axes form a one closed curve.

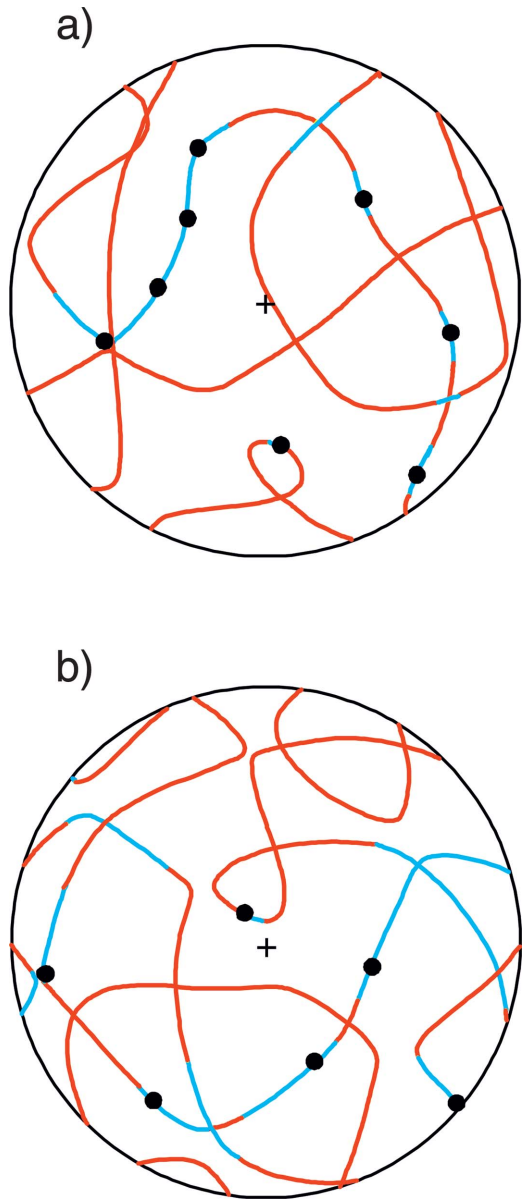

FIG. 6. Directions of real acoustic axes as a function of anisotropy strength for two types of triclinic anisotropy. (a) Anisotropy is described by elasticity tensor (25). (b) Anisotropy is described by elasticity tensor (24). Blue/red lines denote the acoustic axes of stable/unstable media. Black dots mark the positions of acoustic axes for infinitesimally weak anisotropy ($\varepsilon \to 0$), the plus sign marks the vertical axis. Equal-area projection is used.

ACKNOWLEDGMENTS

I thank Vlastislav Červený, Klaus Helbig, and Ivan Pšenčík for stimulating discussions on the subject. The work was supported by the Consortium Project SW3D "Seismic waves in complex 3-D structures," and by the Grant Agency of the Academy of Sciences of the Czech Republic, Grant No. A3012309.

[1]V. I. Alshits and J. Lothe, "Elastic waves in triclinic crystals. I. General theory and the degeneracy problem," Sov. Phys. Crystallogr. **24**, 387–392 (1979).
[2]V. I. Alshits and J. Lothe, "Elastic waves in triclinic crystals. II. Topology of polarization fields and some general theorems," Sov. Phys. Crystallogr. **24**, 393–398 (1979).
[3]V. I. Alshits, A. V. Sarychev, and A. L. Shuvalov, "Classification of degeneracies and analysis of their stability in the theory of elastic waves in crystals" (in Russian), Zh. Eksp. Teor. Fiz. **89**, 922–938 (1985).
[4]A. N. Norris, "Acoustic axes in elasticity," Wave Motion **40**, 315–328 (2004).
[5]A. L. Shuvalov, "Topological features of the polarization fields of plane acoustic waves in anisotropic media," Proc. R. Soc. London, Ser. A **454**, 2911–2947 (1998).
[6]V. I. Alshits and J. Lothe, "Some basic properties of bulk elastic waves in anisotropic media," Wave Motion **40**, 297–313 (2004).
[7]A. G. Every, "Formation of phonon-focusing caustics in crystals," Phys. Rev. B **34**, 2852–2862 (1986).
[8]D. C. Hurley, J. P. Wolfe, and K. A. McCarthy, "Phonon focusing in tellurium dioxide," Phys. Rev. B **33**, 4189–4195 (1986).
[9]A. G. Every, "Classification of the phonon-focusing patterns of tetragonal crystals," Phys. Rev. B **37**, 9964–9977 (1988).
[10]M. R. Hauser, R. L. Weaver, and J. P. Wolfe, "Internal diffraction of ultrasound in crystals: Phonon focusing at long wavelengths," Phys. Rev. Lett. **68**, 2604–2607 (1992).
[11]K. Y. Kim, W. Sachse, and A. G. Every, "Focusing of acoustic energy at the conical point in zinc," Phys. Rev. Lett. **70**, 3443–3446 (1993).
[12]A. L. Shuvalov and G. Every, "Shape of the acoustic slowness surface of anisotropic solids near points of conical degeneracy," J. Acoust. Soc. Am. **101**, 2381–2383 (1997).
[13]J. P. Wolfe, *Imaging Phonons. Acoustic Wave Propagation in Solids* (Cambridge University Press, Cambridge, 1998).
[14]V. Vavryčuk, "Parabolic lines and caustics in homogeneous weakly anisotropic solids," Geophys. J. Int. **152**, 318–334 (2003).
[15]V. Vavryčuk, "Ray tracing in anisotropic media with singularities," Geophys. J. Int. **145**, 265–276 (2001).
[16]V. Vavryčuk, "Behavior of rays near singularities in anisotropic media," Phys. Rev. B **67**, 054105 (2003).
[17]C. H. Chapman and P. M. Shearer, "Ray tracing in azimuthally anisotropic media. II. Quasi-shear wave coupling," Geophys. J. **96**, 65–83 (1989).
[18]R. T. Coates and C. H. Chapman, "Quasi-shear wave coupling in weakly anisotropic 3-D media," Geophys. J. Int. **103**, 301–320 (1990).
[19]Yu. A. Kravtsov and Yu. I. Orlov, *Geometrical Optics of Inhomogeneous Media* (Springer, Berlin, 1990).
[20]V. Červený, *Seismic Ray Theory* (Cambridge University Press, Cambridge, 2001).
[21]P. Bulant and L. Klimeš, "Comparison of quasi-isotropic approximations of the coupling ray theory with the exact solutions in the 1-D anisotropic oblique twisted crystal model," Stud. Geophys. Geod. **48**, 97–116 (2004).
[22]G. Rümpker and C. J. Thomson, "Seismic-waveform effects of conical points in gradually varying anisotropic media," Geophys. J. Int. **118**, 759–780 (1994).
[23]A. G. Khatkevich, "Acoustic axes in crystals," Sov. Phys. Crystallogr. **7**, 601–604 (1963).
[24]F. I. Fedorov, *Theory of Elastic Waves in Crystals* (Plenum, New York, 1968).
[25]A. G. Khatkevich, "Classification of crystals by acoustic properties," Sov. Phys. Crystallogr. **22**, 701–705 (1977).
[26]M. J. P. Musgrave, "Acoustic axes in orthorhombic media," Proc. R. Soc. London, Ser. A **401**, 131–143 (1985).
[27]P. Holm, "Generic elastic media," Phys. Scr., T **44**, 122–127 (1992).
[28]B. M. Darinskii, "Acoustic axes in crystals," Crystallogr. Rep. **39**, 697–703 (1994).
[29]Ph. Boulanger and M. Hayes, "Acoustic axes for elastic waves in crystals: Theory and applications," Proc. R. Soc. London, Ser. A **454**, 2323–2346 (1998).
[30]V. G. Mozhaev, F. Bosia, and M. Weihnacht, "Oblique acoustic axes in trigonal crystals," J. Comput. Acoust. **9**, 1147–1161 (2001).
[31]A. Duda and T. Paszkiewicz, "Number of longitudinal normals and degenerate directions for triclinic and monoclinic media," Eur. Phys. J. B **31**, 327–331 (2003).
[32]M. J. P. Musgrave, *Crystal Acoustics* (Holden-Day, San Francisco, 1970).
[33]R. G. Payton, *Elastic Wave Propagation in Transversely Isotropic Media* (Nijhoff, The Hague, 1983).
[34]R. Fröberg, *An Introduction to Gröbner Bases* (Wiley, New York, 1997).
[35]V. Červený, "Inhomogeneous harmonic plane waves in viscoelastic anisotropic media," Stud. Geophys. Geod. **48**, 167–186 (2004).
[36]T. C. T. Ting, *Anisotropic Elasticity. Theory and Applications* (Oxford University Press, New York, 1996).
[37]A. L. Shuvalov, "On the theory of plane inhomogeneous waves in anisotropic elastic media," Wave Motion **34**, 401–429 (2001).